A New Heat Balance for Flow Boiling

Francisco J. Collado and Carlos Monné
Dept. de Ingeniería Mecánica, CPS-B, Universidad de Zaragoza, Zaragoza, 50018, Spain

Antonio Pascau
Dept. de Ciencia Materiales & Fluidos, CPS-C, Universidad de Zaragoza, Zaragoza, 50018, Spain

DOI 10.1002/aic.11231
Published online June 15, 2007 in Wiley InterScience (www.interscience.wiley.com).

Recently, one of the authors suggested calculating void fraction, an essential element in thermal-hydraulics, working with the "thermodynamic" quality instead of the usual "flow" quality. However, the standard heat balance is currently stated as a function of the "flow" quality. Therefore, we should search a new energy balance between the mixture enthalpy, based on "thermodynamic" quality, and the absorbed heat. This work presents the results of such analysis based on accurate measurements of the axial profile of the cross-sectional average void fraction in the region of boiling with subcooling for water at medium and high pressures taken by Moscow Power Institute (MPI) and Argonne National Laboratory (ANL). As main results, we find that, under uniform heat flux, the mixture enthalpy suffers an abrupt reduction of its slope upon passing saturation point, and a new slip ratio could balance heat with such mixture enthalpy. © 2007 American Institute of Chemical Engineers *AIChE J,* 53: 2123–2130, 2007
Keywords: flow boiling, void fraction, quality, slip ratio, heat balance

Introduction

A large number of correlations[1–6] have been proposed for the evaluation of the cross-sectional average volumetric fraction or void fraction of vapor bubbles α, which is of central interest to power and process industries because void fraction significantly affects neutron absorption, heat transfer, and pressure drop in flow boiling.[1–6] Unfortunately, the complex nonequilibrium subcooled region, in which saturated vapor bubbles steadily coexist with subcooled bulk liquid, has prevented to define a coherent expression of the heat balance for subcooled flow boiling.[1–6]

So, for void fraction calculation, the standard expression for the heat balance for this zone, and also for the full boiling region, is the definition of an "equilibrium" quality[1–6] x_{eq} as

$$\underbrace{x_{eq}h_G + (1 - x_{eq})h_F}_{h_{flow}} = q'z + h_{L,i} \Rightarrow x_{eq} = (q'z + h_{L,i} - h_F)/(h_G - h_F), \quad (1)$$

where q' is the uniform heat per unit mass and per unit inlet length (kJ/kg m), z is the axial distance along the heated wall (m), $h_{L,i}$ is the inlet liquid enthalpy (assuming only liquid at the inlet) (kJ/kg), and h_F and h_G are the saturated liquid and saturated vapor enthalpies at the inlet pressure, respectively (kJ/kg). Usually, the kinetic and gravity terms are neglected.[1–6]

It is clear from Eq. 1 that this "equilibrium" quality will take negative values along the subcooled zone, i.e., until liquid reaches saturation ($x_{eq} = 0$). Evidently, a negative quality has no physical sense and it should be merely taken as a good indicator of the relative thermal distance of the subcooled liquid to saturation. After saturation, the "equilibrium" quality now is positive, being also called "flow" quality, x_{flow}.

To relate this "equilibrium" quality with the unknown true local vapor weight fraction, Levy[4] postulated an exponential

This article includes Supplementary Material available from the authors upon request or via the internet at http://www.interscience.wiley.com/jpages/0001-1541/suppmat/.

Correspondence concerning this article should be addressed to F. J. Collado at fjk@unizar.es.

function. Recently, Delhaye et al.[5] have postulated a hyperbolic tangent function. Then, the vapor volumetric fraction is obtained from this true local vapor weight fraction and accepted relationships between vapor weight and volumetric fractions, which were based mainly on the "drift flux" model of Zuber and Findlay.[6] The "drift flux" model, which is considered complex and empirical,[5] treats the different velocities of the two phases defining the so-called "weighted drift" velocity.[5,6]

Alternatively, the difference of velocity between the phases has been classically quantified through the slip ratio S,[1–3] which is defined as the cross-sectional area mean vapor velocity c_G (m/s) divided by the cross-sectional area mean liquid velocity c_L (m/s). Its standard expression[1–3] in function of "flow" quality x_{flow} (so S would be a "flow" slip), void fraction α, and saturated liquid and vapor densities ρ_F and ρ_G, respectively, is

$$S_{flow} = c_G/c_L = [x_{flow}(1-\alpha)\rho_F]/[(1-x_{flow})\alpha\rho_G]. \quad (2)$$

Unfortunately, the better-known correlations for void fraction, which include the calculation of this slip ratio, may show[1] a standard deviation for the prediction of S_{flow} ranging from 30 to 70–80%.

In conclusion, there is a lack of a heat balance expression that directly supplies true local vapor weight fractions from subcooling to boiling, which is also coherent with actual void fraction measurements.

The main novelty of this work is to use classic thermodynamic relationships between vapor weight and volumetric fractions, i.e., to deal with the well known "thermodynamic" quality x_{th}, classically defined as[3]

$$x_{th} = \rho_G\alpha/\rho_m, \quad (3)$$

where ρ_m is the standard mixture density[1–3] of the vapor-liquid mixture (kg/m^3)

$$\rho_m = \alpha\rho_G + (1-\alpha)\rho_L, \quad (4)$$

and ρ_L is the density of the liquid (kg/m^3), which might be subcooled or saturated.

This was first suggested by Bilicki et al.,[7,8] who pointed out that if we are able to accurately measure the void fraction α, indeed, the mixture density, by gamma-ray or X-ray attenuation, its corresponding actual mass fraction—following Thermodynamics—would be the thermodynamic quality x_{th}, and not the "flow" quality x_{flow}. In recent works,[9,10] we have already shown the obvious thermodynamic coherency between the measured void fraction and the "thermodynamic" quality.

The derivation of α in function of x_{th} and the densities of the phases would be immediate from Eqs. 3 and 4

$$\alpha = x_{th}(\rho_L/\rho_G)/[x_{th}(\rho_L/\rho_G) + (1-x_{th})]. \quad (5)$$

Now the key question would be how the uniform applied heat can be related with the mixture enthalpy, h_m, which is also based on the "thermodynamic" quality x_{th}

$$h_m = x_{th}h_G + (1-x_{th})h_L. \quad (6)$$

So that, we compare the axial profile of the thermodynamic mixture enthalpy to the heat input per unit mass. In the previous works,[9,10] it has been already checked that there are, strong discrepancies between this mixture enthalpy increment and the applied heat. However, it has been also found[9,10] that the explicit inclusion of the slip ratio could close the balance between the absorbed heat and the mixture enthalpy increment.

Therefore, here, we check the following relation

$$qz/S_{new} \sim h_m(z). \quad (7)$$

For this comparison, we use two independent data sets, both with uniform heat flux along a vertical duct with upward flow. First, the accurate measurements of the axial profile of the cross-sectional average void fraction in the region of boiling with subcooling, taken by the Moscow Power Institute (MPI) in the 70s,[11] for flow boiling of water at high pressure in round tubes. And second, some of the tabulated data from one series of investigations of the density of steam-water mixtures at medium pressures in rectangular channels carried out by Argonne National Laboratory (ANL) in the 60s.[12]

As major results of this analysis, we find that, under uniform heat flux, the thermodynamic mixture enthalpy suffers an abrupt reduction of its slope upon passing the saturation point. This change of slope could be logically related with the well-known change of curvature of the measured axial profile of void fraction at saturation. Furthermore, a new slip ratio could close the balance between heat and mixture enthalpy. However, there is a strong relation between the new slip ratio and the standard one.

In conclusion, it would be possible an accurate prediction of the void fraction axial profile through the mixture enthalpy, which is based on the thermodynamic quality (see Eqs. 5 and 6), calculated from the new heat balance. So, it would be necessary to know only three parameters for each test in addition to the operational parameters. The first one would be the starting point of the subcooled boiling region, classically defined as the point of net vapor generation[13,14] (PNVG), which in this work will be identified as a PNVG "equilibrium" quality, i.e., $x_{eq\text{-}PNVG}$. The other two ones would be particular values of the new slip ratio namely, the slip ratio at the end of the subcooling region, i.e., just at saturation, and the average of the new slip ratio along full boiling.

MPI measurements of the axial profile of void fraction

Accurate measurements of the axial profile of the void fraction in the region of boiling with subcooling for water at high pressure were carried out in the 70s at MPI for a wide range of severe operating conditions. In the 24 tests reported by Bartolomei et al.,[11] the inlet pressure p_i, mass flux G, and heat flux q'' range from 3.01 to 14.68 MPa, from 405 to 2123 kg m^{-2} s^{-1} and from 0.42 to 2.21 MW m^{-2}, respectively.

The experimental upward channels were made up of commercial tubes 12×10^{-3} m of internal diameter and 2×10^{-3} m of wall thickness, with heated lengths from 0.8 to 1.5 m. Maximum relative errors within the entire range of investigations did not exceed 0.01 for pressure, 0.02 for mass veloc-

Table 1. Conditions of the Tests Presented by Bartolomei et al.[11]

O. P. Varied	No. Test	p_i (MPa)	G (kg/m^2 s)	q'' (MW/m^2)	$\Delta T_{sub,I}$ (°C)	$c_{L,I}$ (m/s)	$x_{eq\text{-}PNVG}$	$S_{1,sat}$	S_2	$\alpha_{o,mea}$	$\alpha_{o,cal}$
none	1-1	6.89	985	1.13	93.9	1.12	−0.1	0.936	2.99	0.490	0.486
	1–2	6.78	1071	1.13	91.8	1.22	−0.13	0.921	2.19	0.538	0.523
	1–3	6.84	961	1.13	91.4	1.10	−0.12	0.927	2.29	0.590	0.587
	1–4	6.84	995	1.15	91.4	1.13	−0.10	0.927	2.48	0.585	0.556
q''	2a-1	6.81	998	0.44	36.1	1.24	−0.05	0.93	2.17	0.296	0.297
	2a-2	6.89	965	0.78	64.9	1.14	−0.08	0.905	2.29	0.488	0.487
	2a-3	6.84	961	1.13	91.4	1.10	−0.12	0.927	2.29	0.590	0.587
	2a-4	6.74	988	1.7	140.4	1.07	−0.13	0.938	2.41	0.575	0.573
	2a-5	7.01	996	1.98	125.1	1.09	−0.15	0.935	3.34	0.463	0.458
q''	2b-1	14.79	1878	0.42	11.2	2.89	−0.03	0.906	(3.74)	0.067	0.087
	2b-2	14.74	1847	0.77	15.9	2.78	−0.1	0.900	1.35	0.350	0.348
	2b-3	14.75	2123	1.13	31.0	3.02	−0.12	0.891	1.35	0.288	0.289
	2b-4	14.70	2014	1.72	68.7	2.59	−0.12	0.911	(4.4)	0.216	0.216
	2b-5	14.99	2012	2.21	52.3	2.70	−0.18	0.863	–	0.185	0.185
G	3a-1	6.89	405	0.79	136.9	0.44	−0.14	0.925	2.56	0.600	0.598
	3a-2	6.89	965	0.78	64.9	1.14	−0.08	0.905	2.29	0.488	0.487
	3a-3	6.89	1467	0.77	38.9	1.81	−0.09	0.909	–	0.175	0.173
	3a-4	6.79	2024	0.78	36.9	2.51	−0.04	0.900	–	0.225	0.225
G	3b-1	11.02	503	0.99	97.4	0.59	−0.19	0.910	1.69	0.550	0.540
	3b-2	10.81	966	1.13	87.9	1.16	−0.15	0.906	1.99	0.490	0.498
	3b-3	10.81	1554	1.16	26.9	2.1	−0.12	0.795	1.70	0.488	0.489
	3b-4	10.84	1959	1.13	27.1	2.65	−0.07	0.875	1.40	0.508	0.518
p_i	4a-1	3.01	990	0.98	62.2	1.1	−0.06	0.960	2.86	0.49	0.490
	4a-2	4.41	994	0.90	66.4	1.13	−0.09	0.930	2.74	0.586	0.570
	4a-3	6.84	961	1.13	91.4	1.10	−0.12	0.927	2.29	0.59	0.587
	4a-4	10.81	966	1.13	87.9	1.16	−0.15	0.906	1.99	0.490	0.498
	4a-5	14.68	1000	1.13	80.6	1.26	−0.20	0.879	1.86	0.458	0.442
p_i	4b-1	6.81	2037	1.13	53.1	2.45	−0.05	0.917	(2.98)	0.283	0.283
	4b-2	10.84	1959	1.13	27.1	2.65	−0.07	0.875	1.40	0.508	0.518
	4b-3	14.75	2123	1.13	31.0	3.02	−0.12	0.891	1.35	0.288	0.289

ity, 0.03 for heat flux density, and 1 K for temperature. The main investigated parameter was the true volumetric steam content α—determined by penetrating γ-radiation—whose maximum absolute error did not exceed ± 0.04.

In Table 1, the characteristics of the 24 MPI tests are shown. They have been gathered and named following the number of the figures and the increase of the operational parameter (O. P.) varied.[11] The shaded tests, although repeated, are included to analyze the influence of heat flux, mass velocity, and pressure in the model. Recently, Delhaye et al.[5] have used the same MPI data as reference to validate some extrapolations from R12 void fraction data to water at high pressure, due to the high expense of such experiments.

New heat balance

In the work of Bartolomei et al.,[11] axial profiles of the measured local cross-sectional average void fraction are presented versus the measured relative enthalpy (or "equilibrium" quality; Eq. 1). To define the new heat balance, we compare the axial profile of the mixture enthalpy h_m (Eq. 6) with that of the standard heat balance, i.e., $q'z + h_{L,i}$. Previously, to obtain h_m from data, we need to establish some basic assumptions about the thermodynamic properties used.

First, we neglect pressure drop, so assuming a constant pressure along the channel equal to the inlet pressure p_i. For the liquid enthalpy at subcooling, we assume the classic approach[1,2] of considering it practically equal to the "flow" mixture enthalpy, i.e., Eq. 1,

$$h_L \approx q'z + h_{L,i} \Rightarrow h_F = q'z_{sat} + h_{L,i} \Rightarrow z_{sat} = \left(h_F - h_{L,i}\right)/q'. \tag{8}$$

So, the axial location of the saturation point z_{sat} can be readily calculated. The saturation properties of the liquid and vapor have been read in thermodynamic tables entering with inlet pressure, whereas the subcooled liquid properties have been obtained entering with the above-calculated subcooled liquid enthalpy and the inlet pressure.

The actual axial distance z has been easily derived entering in Eq. 1 with the "equilibrium" quality x_{eq}, extracted from the figures and the applied heat flux reported.[11] Finally, the local mixture density (Eq. 4), is calculated from the void fraction data and the above-commented thermodynamic properties, and so the thermodynamic quality x_{th} (Eq. 3), which finally allows the calculation of $h_m(z)$ (Eq. 6).

Figure 1 shows $h_m(z)$ for test 1–3 (see Table 1), which is identical to tests 2a-3 and 4a-3. The circles represent the thermodynamic mixture enthalpy (Eq. 6), from the reduced data, the triangles represent the liquid enthalpy profile $h_L(z)$, from Eq. 8, and the fine line represent the standard heat balance $q'z + h_{L,i}$. The bold line is the simulation procedure followed in this work, which will be commented later.

Logically, with the assumptions made, the mixture enthalpy along subcooling (Eq. 6), is greater than the subcooled liquid enthalpy. However, in reaching saturation, the mixture enthalpy suffers such an abrupt reduction of its slope that it may be even below the standard heat balance. This dramatic change of slope of the mixture enthalpy would be clearly

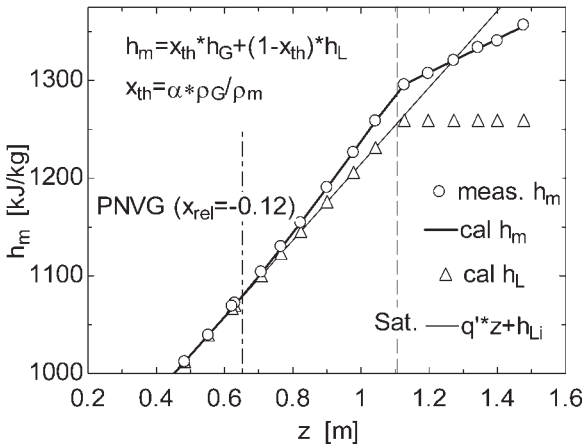

Figure 1. Mixture enthalpy vs. *z* for test 1–3 (MPI).

justified for the strong but well-known change suffered by the liquid enthalpy of a pure substance under heating upon passing the saturation point, i.e., from growing values of $h_L(z)$ along subcooling to a practically constant value h_F at full saturated boiling (neglecting pressure drop changes).

This behavior of the mixture enthalpy $h_m(z)$—rather different from the classic "flow" enthalpy or standard heat balance i.e., $q'z + h_{L,i}$, has been definitely confirmed for the 24 tests in Table 1, see Figures 1a–7a in the supplementary material, and for the 31 ANL tests presented later in Table 2, see Figures 8a–13a in the supplementary material. Furthermore, this clear change of the mixture enthalpy slope in passing saturation has been also recently verified for some general electric tests with low-pressure water.[15] Notice that, under uniform heat release along the channel, classic treatments cannot explain at all this marked, although physically justified, change of enthalpy slope.

The authors have already suggested elsewhere[9,10,15] to explicitly include the slip ratio in a new heat balance (Eq. 7). Of course, this new included parameter could balance heat input with mixture enthalpy.

Furthermore, the strong change of slope between subcooling and saturated boiling would suggest using two different slip ratios namely, S_1 for the subcooled zone, just until the saturation point, and S_2 for the full boiling region. Then, at subcooling, the new suggested heat balance would be

$$h_m = q'z/S_1 + h_{L,i} \Rightarrow S_1 = q'z/\left(h_m - h_{L,i}\right). \tag{9}$$

After saturation, the evolution of the mixture enthalpy should be a continuation of the former one

$$h_m = q'\left(z - z_{sat}\right)/S_2 + h_{m,sat} \Rightarrow S_2 = q'(z - z_{sat})/\left(h_m - h_{m,sat}\right). \tag{10}$$

So, in Eq. 10, the mixture enthalpy at the saturation point, at the end of subcooling, is derived from Eq. 9, also including Eq. 8,

$$h_{m,sat} = q'z_{sat}/S_{1,sat} + h_{L,i} = \left(h_F - h_{L,i}\right)/S_{1,sat} + h_{L,i}. \tag{11}$$

Table 2. Conditions of Some of the Tests Presented by Marchaterre et al.[12]

No. Test	p_i (MPa)	G (kg/m^2 s)	q'' (MW/m^2)	$\Delta T_{sub,i}$ (°C)	$c_{L,i}$ (m/s)	$x_{eq\text{-}PNVG}$	$S_{1,sat}$ (*ave)	$S_{2,ave}$	$\alpha_{o,mea}$	$\alpha_{o,cal}$
236	1.12	406	0.12	5.4	0.46	−0.006	0.916*	3.21	0.600	0.626
234	1.12	527	0.12	4.1	0.59	−0.006	0.900*	2.88	0.570	0.591
231	1.13	674	0.12	3.2	0.76	−0.005	0.900*	2.55	0.545	0.557
230	1.13	733	0.12	5.4	0.83	−0.004	0.885*	2.40	0.550	0.552
228	1.12	380	0.15	7.3	0.43	−0.014	0.874	3.9	0.660	0.658
225	1.12	500	0.15	5.1	0.56	−0.010	0.890*	3.57	0.600	0.609
222	1.12	683	0.15	4.3	0.77	−0.008	0.868*	2.78	0.570	0.585
217	1.12	475	0.20	7.6	0.53	−0.012	0.896*	3.5	0.630	0.688
213	1.12	670	0.20	4.8	0.76	−0.008	0.850*	2.7	0.68	0.678
212	1.12	729	0.20	4.2	0.82	−0.008	0.845*	2.6	0.675	0.669
209	1.12	473	0.25	9.0	0.53	−0.013	0.889*	3.28	0.710	0.750
207	1.12	578	0.25	7.8	0.65	−0.013	0.896*	2.95	0.710	0.725
206	1.12	645	0.25	6.9	0.73	−0.013	0.862*	2.75	0.725	0.724
203	1.80	434	0.15	6.3	0.50	−0.014	0.895*	2.70	0.550	0.588
201	1.82	604	0.15	4.8	0.70	−0.011	0.845	2.60	0.515	0.525
247	1.81	789	0.15	3.3	0.92	−0.008	0.857*	2.50	0.480	0.469
199	1.81	417	0.20	8.6	0.48	−0.020	0.890	3.40	0.595	0.623
197	1.82	459	0.20	7.9	0.53	−0.017	0.865	3.30	0.640	0.614
189	1.81	621	0.20	5.8	0.72	−0.010	0.854*	2.95	0.560	0.567
193	1.82	377	0.25	13.4	0.43	−0.030	0.905	3.1	0.680	0.703
192	1.81	453	0.25	10.3	0.52	−0.020	0.870*	3.00	0.695	0.686
190	1.81	601	0.25	7.7	0.69	−0.015	0.865*	2.80	0.650	0.636
168	4.23	329	0.15	11.6	0.41	−0.030	0.895	3.00	0.390	0.401
167	4.23	404	0.15	8.9	0.50	−0.025	0.890	2.95	0.375	0.362
153	4.24	708	0.15	4.8	0.88	−0.012	0.859*	2.76	0.295	0.269
173	4.23	289	0.20	15.9	0.35	−0.030	0.915	3.5	0.480	0.476
172	4.23	362	0.20	12.7	0.45	−0.030	0.880	3.38	0.440	0.444
154	4.22	722	0.20	5.9	0.90	−0.012	0.872	2.84	0.350	0.322
187	4.23	380	0.25	14.0	0.47	−0.040	0.94	3.25	0.460	0.475
186	4.23	458	0.25	12.2	0.56	−0.030	0.905	3.16	0.420	0.446
183	4.23	743.8	0.25	7.6	0.92	−0.020	0.880	2.79	0.35	0.363

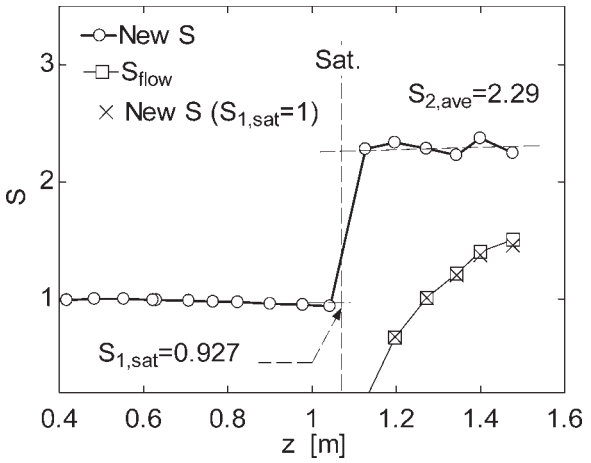

Figure 2. New slip ratio vs. *z* for test 1–3 (MPI).

Now, substituting Eq. 11 in Eq. 10, we obtain

$$S_2 = \left\lfloor q'z - \left(h_F - h_{L,i}\right)\right\rfloor / \left\lfloor h_m - h_{L,i} - \left(h_F - h_{L,i}\right)/S_{1,sat}\right\rfloor. \tag{12}$$

Finally, by convenience, we derive an approximation to S_2, see Eq. 12, assuming that $S_{1,sat} \approx 1$

$$S_2\left(S_{1,sat} \approx 1\right) = \left\lfloor q'z - \left(h_F - h_{L,i}\right)\right\rfloor / \left(h_m - h_F\right). \tag{13}$$

New slip ratio

Figure 2 presents the axial profiles of S_1, along subcooling, and S_2, along full boiling, Eqs. 9 and 12, respectively, for test 1–3. Starting at one, i.e., single flow, S_1 goes down smoothly until reaching saturation $S_{1,sat} = 0.927$. As this slip ratio is less than one, the mixture enthalpy can be greater than the standard one (see Eq. 9). This new slip ratio cannot take negative values, and its order of magnitude, slightly less than one, would be confirmed by historic photographic measurements of vapor bubble velocity at subcooling.[1,2]

After saturation, the new suggested slip ratio S_2 (Eq. 10), is definitely greater than one, although now, at difference from S_1, S_2 would be practically constant along saturated boiling. This would justify taking a constant value for the saturation region equal to the arithmetic average of their calculated values from Eq. 12 along full boiling. As we will see later, the good predictions of the void fraction in this region, not only for MPI tests but also for ANL ones, would also support this average.

To indirectly check that this new parameter S_2 is actually a slip ratio, we have compared the classic "flow" slip ratio S_{flow} (Eq. 2), with an approximation to the new S_2, i.e., Eq. 13, in which we have assumed that $S_{1,sat} \approx 1$ along saturation. We have plotted them starting at saturation because S_{flow} would take negative values at subcooling with the classic procedure (see Eq. 2).

As can be seen in Figure 2, the coincidence between them is very strong. Also note that the slight change from $S_{1,stat} = 0.927$ to $S_{1,sat} \approx 1$ means a completely different shape profile along saturation. The behavior of the new slip ratio and the comparison between the classic slip ratio and such approximation to the new one can be seen in Figures 1b–7b in the supplementary material for the 24 tests in Table 1. Also, refer to Figures 8b–13b in the supplementary material for the 31 ANL tests of Table 2.

Finally, note that the authors have recently verified elsewhere[9] the new suggested heat balance (Eq. 7), finding a quite strong relation between the classic slip ratio and the heat-mixture enthalpy ratio, although there for saturated flow boiling, which entered in the heated channel exactly as saturated liquid without vapor, i.e., $S_{1,sat} \approx 1$.

Void fraction prediction

The new procedure suggested here for calculating void fraction needs for values of S_1 and S_2. As we have commented earlier, we will take a constant value for S_2. However, for S_1, we will assume a simple linear decay from $S_1 = 1$ at the starting point of boiling until saturation $S_1 = S_{1,sat}$, i.e.,

$$S_1 \approx 1 + \left(S_{1,sat} - 1\right)\left(z - z_{PNVG}\right)/\left(z_{sat} - z_{PNVG}\right), \tag{14}$$

where the axial position of the beginning of boiling or "point of net vapor generation"[13,14] (PNVG) has been denoted here by z_{PNVG}. By the sake of convenience, instead of directly searching the axial distance z_{PNVG}, first it has been checked the corresponding relative enthalpy value, denoted by $x_{eq\text{-}PNVG}$ in Table 1, which better fitted the void fraction in the subcooled region. Then, the derivation of z_{PNVG}, necessary for Eq. 14, is immediate entering in Eq. 1 with $x_{eq\text{-}PNVG}$.

Now, we are capable of reproducing the heat balance, i.e., the axial profile of the thermodynamic mixture enthalpy, provided we have the right two slip ratios, i.e., $S_{1,sat}$ and $S_{2,ave}$, and the location of the PNVG or $x_{eq\text{-}PNVG}$. So, the bold line in Figure 1 is the simulated axial profile of such mixture enthalpy. Then, from the definition of h_m (Eq. 6), we can calculate the thermodynamic quality x_{th} and, finally, from Eq. 5, the void fraction is calculated.

Figure 3 compares the measured axial profile of the void fraction with the calculated one following this new procedure for test 1–3 in Table 1. The model fails in the first region of subcooling, with very low values of the void fraction.

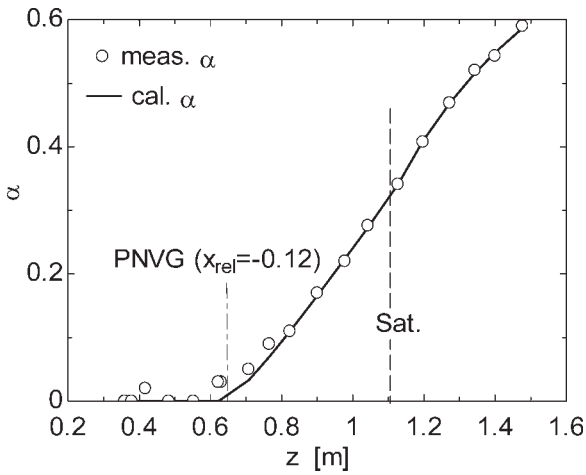

Figure 3. Void fraction vs. *z* for test 1–3 (MPI).

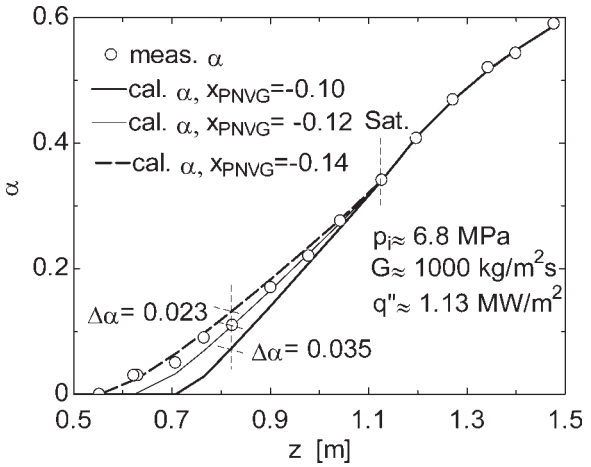

Figure 4. Void fraction sensitivity to $x_{eq\text{-}PNVG}$ for tests 1–3 (MPI).

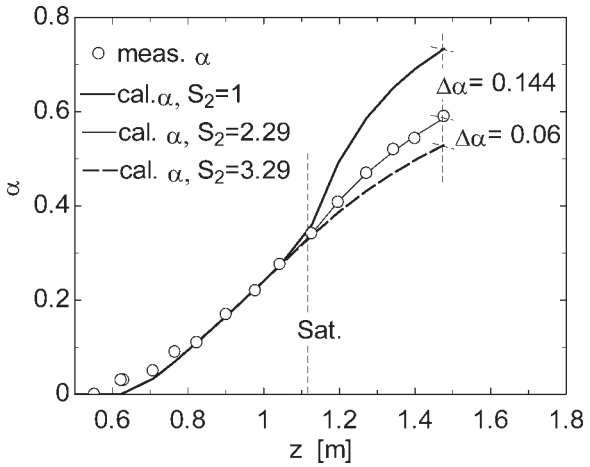

Figure 6. Void fraction sensitivity to S_2 for test 1–3 (MPI).

Although for the second region, i.e., fully developed subcooled boiling[14] and the full saturation zone, the agreement is quite acceptable.

The comparison between the measured and calculated axial profiles of the void fraction for the MPI set of 24 tests analyzed (Table 1) can be found in Figures 1c–7c in the supplementary material. The values of the two slip ratios and the PNVG that better fit the axial void fraction profile data are shown in Table 1. Also, refer to Figures 8c–13c in the supplementary material and Table 2.

Finally, Figures 4–6 show some partial sensitivity analysis of the void fraction calculation to variations on the three main parameters of the model, respectively, i.e., the new slip ratios and the PNVG for test 1–3 in Table 1, at 6.8 MPa. So, a decrease of 0.03 in $S_{1,sat}$ could imply a calculated void fraction absolute difference with data of about 0.08; although an increase of 0.03, thus approaching to one, i.e., to the classic heat balance, would mean about a 0.19 of absolute error. By the other side, an increase of 1.0 in S_2 would only provoke an absolute decrease of 0.06. Furthermore, it has been checked that with $S_2 = 1$, i.e., using the classic heat balance expression although including the thermodynamic enthalpy, the void fraction calculated exhibit a difference of about 0.14 with data. Finally, it would seem that the sensitivity of void fraction calculation at subcooling is not too high to variations of the PNVG. So, reductions or increases of such point value by 0.02 would mean about 0.02–0.04 of net difference, respectively, with void fraction data at fully developed subcooled region.

ANL measurements of the axial profile of void fraction

Accurate measurements of the axial profile of the void fraction in the region of boiling with subcooling for water at medium pressure (1.12–4.23 MPa) and low subcooling were carried out in the 60s at the ANL for a wide range of severe operating conditions. The data, reported by Marchaterre et al.,[12] were taken for natural and forced circulation in 12.7 $\times 10^{-3} - 6.35 \times 10^{-3}$ m (0.5–0.25 in.) by 50.8×10^{-3} m (2 in.) by 1.524 m (60 in.) rectangular channels over a veloc-

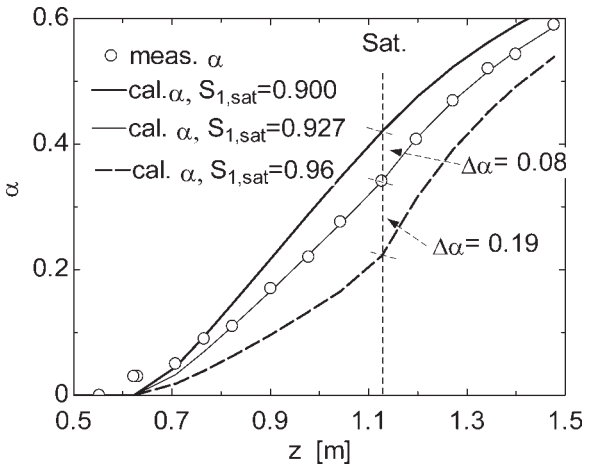

Figure 5. Void fraction sensitivity to $S_{1,sat}$ for test 1–3 (MPI).

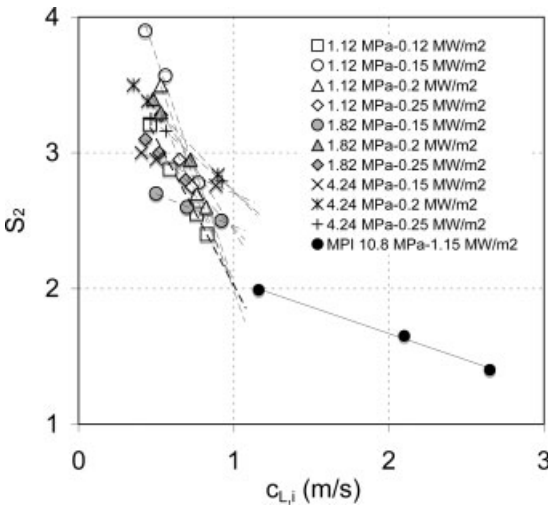

Figure 7. S_2 versus inlet liquid velocity: ANL tests.

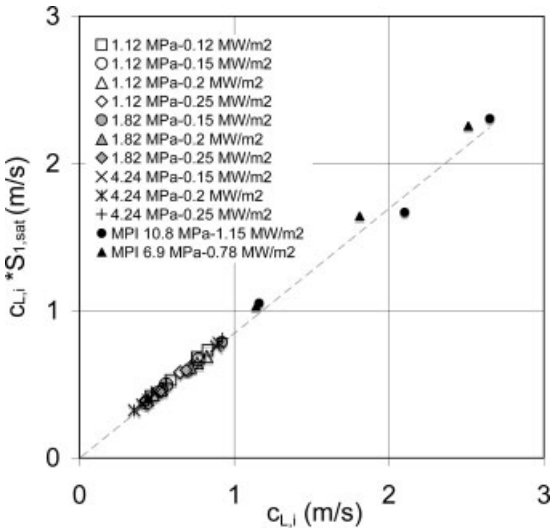

Figure 8. $S_{1,sat}$*$c_{L,i}$ vs. inlet liquid velocity: ANL tests.

ity range of 0.305–1.83 m/s, and a "flow" quality range of 0–6%.

From the tests reported for the wider channel, i.e., 12.7×10^{-3} m, we have selected, see Table 2, for the different pressures, 31 tests in which the inlet velocity was varied, but keeping constant the heat flux. The name of the tests in Table 2 is the same as reported.[12] So, Figures 8a–15a in the supplementary material represent the mixture enthalpy profile, Figures 8b–13b in the supplementary material show the new slip ratio profile, and Figures 8c–13c in the supplementary material compare the calculated and measured void fraction. The behavior and trends of the new variables is identical to the MPI tests, which would confirm the new heat balance.

Conclusions

The main novelty of this work about flow boiling is to use classic thermodynamic relationships between vapor weight and volumetric fractions, i.e., to deal with the well-known thermodynamic quality.

Using accurate and independent void fraction data sets[11,12] measured under uniform heat flux, we define a mixture enthalpy, based on the thermodynamic quality, which suffers a dramatic change of slope upon passing the saturation point. This would be logically connected with the well-known change of the liquid enthalpy of a pure substance in passing upon saturation point. The measured void fraction[16] also suffers a change of curvature in passing saturation.

In the new energetic expression proposed here, the absorbed heat is balanced with such thermodynamic mixture enthalpy through a new slip ratio, which is closely related to the classic "flow" slip ratio. An intuitive explanation of this slip ratio inclusion could be the physical fact that the mean vapor bubbles velocity is different from the subcooled or saturated bulk liquid velocity. Velocity being a space-time ratio, if we are treating simultaneously these two different velocities along the same distance, i.e., the same control volume, their time scales should be also different. Therefore, the slip ratio would act as a scaling time factor between the two phases. Heat would enter into the control volume through the condensing vapor bubbles—as long as the heated wall is completely covered of bubbles,[14] with a time scale different from the inlet bulk liquid.

With the new heat balance proposed here, the accurate calculation of the axial profile of the void fraction would be based on three parameters namely, the PNVG expressed as an "equilibrium" quality value, the new slip ratio just at saturation $S_{1,sat}$ (less than unity although close to it, 0.85–0.94) and an average value of the new slip ratio along full saturation S_2, which is definitely greater than one (1.4–3.8 for the tests analyzed here).

There are strong experimental evidences of the constancy of the new slip ratio along full saturation S_2. As more uniform S_2 is more regular the axial profile of void fraction is. Even for the tests in which S_2 suffers strong oscillations along the channel, the average value gives good approximations to the experimental void fraction data. For some ANL tests at the lowest pressure and subcooling, there are also indications of that S_1 is practically constant, see tests with asterisk in Table 2.

About the dependence of the new slip ratio parameters with the main operational parameters namely, inlet pressure, heat flux, and inlet velocity, it would be clear, from Tables 1 and 2, a logic and very clear dependence of $S_{1,sat}$ and S_2 on the liquid inlet velocity $c_{L,i}$. So, higher the inlet velocity is, the lower both new slip ratios are. About pressure, Figure 6b in the supplementary material would show that S_2 diminishes with increasing pressure. About heat flux, the trends of the new slip ratios are not so clear.

Finally, as a first approximation to the calculation of the new slip ratios in function of the main operational parameters, we have represented S_2 in function of the inlet velocity for different pressures and heat fluxes, see Figure 7; whereas, based on a previous work,[9] we have plotted $c_{L,i}$*$S_{1,sat}$ vs. $c_{L,i}$ (see Figure 8). Watching such linear plots, it seems possible to accurately fit these key parameters. Work is in progress.

Acknowledgments

The authors thank the Spanish Minister of Education and Science (MEC) the funding of this research through the research project DPI2005-08654-C04-04.

Literature Cited

1. Collier JG. Nuclear steam generators and waste heat boilers. In Kakaç S, editor. *Boilers, Evaporators and Condensers*. New York: Wiley, 1991: Chapter 9.
2. Collier JG, Thome JR. *Convective Boiling and Condensation*, 3rd ed. Oxford, UK: Oxford University Press, 1994.
3. Lahey RT Jr, Moody, FJ. *The Thermal Hydraulics of a Boiling Water Nuclear Reactor*. La Grange Park: American Nuclear Society, 1979.
4. Levy S. Forced convection subcooled boiling-prediction of vapor volumetric fraction. *Int J Heat Mass Transf*. 1967;19:99–113.
5. Delhaye JM, Maugin F, Ochterbeck JM. Void fraction predictions in forced convective subcooled boiling of water between 10 and 18 MPa. *Int J Heat Mass Transf*. 2004;47:4415–4425.
6. Zuber N, Findlay JA. Average volumetric concentration in two phase flow systems. *ASME J Heat Transf*. 1965;87:453–467.

7. Bilicki Z, Michaelides EE. Thermodynamic nonequilibrium in liquid-vapour flows. *J Non-Equil Therm*. 1997;22:99–109.
8. Bilicki Z, Giot M, Kwidzinski R. Fundamentals of two-phase flow by the method of irreversible thermodynamics. *Int J Multiphase Flow*. 2002;28:1983–2005.
9. Collado FJ, Monné C, Pascau A, Fuster D, Medrano A. Thermodynamics of void fraction in saturated flow boiling. *J Heat Transf-Trans ASME*. 2006;128:611–615.
10. Collado FJ, Monné C, Pascau A. A new heat balance for flow boiling. *Proceedings of 2006 AIChE Annual Meeting*, November 12–17. San Francisco: AIChE, 2006.
11. Bartolomei GG, Brantov VG, Molochnikov YuS, Kharitonov YuV, Solodkii VA, Batashova, GN, Mikhailov VN. An experimental investigation of true volumetric vapour content with subcooled boiling in tubes. *Therm Eng*. 1982;29:132–135.
12. Marchaterre JF, Petrick M, Lottes PA, Weatherhead RJ, Flinn WS. *Natural and Forced-Circulation Boiling Studies*. Chicago: Argonne National Laboratory, ANL-5735, 1960.
13. Saha P, Zuber N. Point of net vapor generation and vapor void fraction in subcooled boiling. *Proceedings of the Fifth International Heat Transfer Conference*, Tokio, 1974: paper B4.7.
14. Griffith P, Clark JA, Rohsenow, WM. *Void Volumes in Subcooled Boiling Systems*. New York: ASME, 1958: paper 58-HT-19.
15. Collado FJ, Monné C, Pascau A. Changes of enthalpy slope in subcooled flow boiling. *Heat Mass Transf*. 2006;42:437–448.
16. Ahmad, SY. Axial distribution of bulk temperature and void fraction in a heated channel with inlet subcooling. *J Heat Transf-Trans ASME*. 1970;92:595–609.

Manuscript received Nov. 4, 2006, and revision received Apr. 23 2007.